SPECIAL PUBLICATION OF THE GEOLOGICAL SOCIETY OF INDIA
No.13, 2026, pp. 389–400

Lithium Potential in LCT Pegmatites of Mangalur Schist Belt, Eastern Dharwar Craton, India

M. Satyanarayanan[1, 2*], K. Thillairaj[3], G. Parthasarathy[3,4], C. S. Sindhuja[1,2], Ajay Kumar Singh[1,2] and Dheeraj Pande[5]

[1]CSIR-National Geophysical Research Institute, Uppal Road, Hyderabad-500007, India
[2]Academy of Scientific & Innovative Research, Ghaziabad-201002, India
[3]Atomic Minerals Directorate for Exploration & Research (AMD), Nagarabhavi, Bengaluru-560072, India
[4] School of Natural and Engineering Sciences, National Institute of Advanced Studies, Indian Institute of Science Campus, Bengaluru-560012, India
[5]Atomic Minerals Directorate for Exploration & Research (AMD), Begumpet, Hyderabad-500016, India
***E-mail**: msnarayanan.ngri@csir.res.in*
Received 14 July 2026; Revised 30 August 2026; Accepted 31 August 2026

Abstract: We present the petrography and whole-rock geochemistry of lithium-bearing pegmatites from the Mangalur Schist Belt (MSB), located along the western margin of the Eastern Dharwar Craton (EDC), India, to constrain their petrogenesis, rare-metal enrichment and mineralization processes. Although the MSB has received comparatively little attention relative to adjacent lithium-bearing pegmatite near Amareshwar in Gurgunta Schist Belt, its geological setting provides an opportunity to evaluate the evolution of rare-element pegmatites within the Eastern Dharwar Craton and their significance for India's growing demand for critical minerals resources. The late Archean pegmatites intrude the volcano-sedimentary sequence of the MSB and comprise coarse-grained, holocrystalline assemblages dominated by quartz, plagioclase, microcline, biotite and spodumene. Petrographic studies reveal graphic intergrowths and recrystallized quartz exhibiting undulose extinction and overgrowth, indicating late-stage eutectic crystallization followed by post-emplacement deformation. SEM-EDS analyses confirm the presence of primary fluorapatite within the interstitial quartz-feldspar matrix, indicating that the parental melt was enriched in phosphorus and fluorine bearing volatile fluxes. Whole-rock trace element geochemistry reveals a highly evolved Lithium–Cesium–Tantalum (LCT) affinity, consistent with derivation from a fertile, peraluminous S-type granitic magma through extensive fractional crystallization, characterized by enrichment in Li (whole-rock up to 97 ppm; spodumene bearing samples containing 5.6–6.1 wt.%), Rb (up to 1698 ppm), and Cs (up to 119 ppm), together with depletion of Ba (31–48 ppm) and Sr (6–16 ppm), reflecting extensive fractionation of feldspar during magmatic evolution. Systematically low Nb/Ta (~2.6) and Zr/Hf (~15.7) ratios further record magmatic differentiation and late-stage magmatic–hydrothermal evolution. We infer that progressive enrichment of fluorine- and phosphorus-bearing volatiles reduced melt viscosity and depressed the solidus temperature, thereby delaying fractional crystallization and influencing the concentration of lithium and other incompatible elements in the residual melt prior to its emplacement into structurally controlled fractures within the MSB. These results show the MSB pegmatites as highly evolved LCT-type systems, and highlight their potential as an emerging lithium resource within the Eastern Dharwar Craton, with implications for Li, Nb and Ta exploration.

Keywords: Lithium; Pegmatite; Geochemistry; Mangalur Schist Belt; Dharwar Craton.

Recommended Citation:
Satyanarayanan, M., Thillairaj, K., Parthasarathy, G., Sindhuja, C.S., Singh, Ajay Kumar, and Pande, Dheeraj (2026). Lithium Potential in LCT Pegmatites of Mangalur Schist Belt, Eastern Dharwar Craton, India. In: *Natural Resources and their Utilisation with Special Reference to Critical Minerals* (Ed.: Mohanty, S.P.). Special Publication of the Geological Society of India (Bengaluru), 13, id:174506. https://doi.org/10.17491/CGSI.2026.174506

INTRODUCTION

The Archean greenstone belts of the Eastern Dharwar Craton (EDC), southern India, have traditionally been investigated for their significant gold and base-metal mineralization (Curtis and Radhakrishna, 1993; Radhakrishna and Vaidyanadhan, 1997; Sawkar et al., 1999; Naqvi et al., 2008). In recent years, however, increasing attention has been directed toward their potential to host critical metal in pegmatite systems enriched in strategic commodities such as lithium (Li), cesium (Cs), and tantalum (Ta). This renewed interest is driven by rapidly expanding demand for critical minerals required for energy storage technologies and the global transition toward clean energy (Greim et al., 2020). Granitic pegmatites are among the most important primary sources of Li, accounting for more than 30% of the global supply to lithium-based industries (Su et al., 2019; Balaram et al., 2024; Pandey, 2025), though lithium bearing minerals such as Cookeite ($LiAl_4(Si_3Al)O_{10}(OH)_8$) has been reported from sedimentary formation in India (Saikia et al., 2026). Although it is widely distributed in granitic pegmatites, deposits containing economically viable concentrations are relatively rare and occur as discrete pockets. It has been estimated that fewer than 3% of granitic pegmatites within a typical pegmatite province contain lithium or other rare-element mineralization of sufficient grade and tonnage for commercial extraction (Černý and Ercit, 2005; London, 2008; Černý et al., 2012).). Consequently, the increasing demand for Li and other critical metals has significantly enhanced the exploration and economic importance of rare-element pegmatites as high-grade mineral resources (Grosjean et al., 2012; Kesler et al., 2012; Linnen et al., 2012; Maneta and Baker, 2017; Balaram et al., 2024).

In India, investigations of lithium-bearing pegmatites have recently focused on the Amareshwar area of the Gurgunta Schist Belt, EDC, where spodumene-bearing pegmatites were first documented by Devaraju et al. (1990). Subsequent beneficiation studies established the suitability of these lithium-bearing pegmatites for downstream processing (Kundu et al., 2023 a, b), culminating in the preparation of lithium-ion battery materials at CSIR–CECRI, Karaikudi, Tamil Nadu *(personal communication)*. In contrast, the rare-metal potential of the Mangalur Schist Belt (MSB), located about 50 km north of Amareshwar, has remained comparatively underexplored despite similarity in geological setting and the occurrence of gold mineralization in both regions (Rao, 1980). Accordingly, this study presents a comprehensive investigation of the pegmatites in the Mangalur Schist Belt to geochemically characterize, evaluate, and identify the controls on mineralization, and constrain their genetic evolution.

GEOLOGICAL SETTING

The Mangalur Schist Belt (MSB) is situated along the western margin of the Eastern Dharwar Craton (EDC), a prominent Neoarchean crustal block in southern India. The EDC is characterized by elongated, structurally complex greenstone belts dominated by metavolcanic and metasedimentary sequences, enveloped by younger intrusive granites (Manikyamba and Kerrich, 2012; Jayananda et al., 2013; Peucat et al., 2013). The MSB itself represents a distinct litho-tectonic unit, primarily composed of mafic-ultramafic volcanic rocks, banded iron formations (BIF), and associated metasediments (Tenginkai and Ugarkar, 1987; Ugarkar and Tenginkai, 1988, 1989). The pegmatites in the study area occur as a swarm of discordant, tabular bodies intruding the core and margins of the MSB south of the Mugankavi gold mine, and located to the south of the Neoproterozoic Bhima basin in Yadgir district, Karnataka. Geologically, the area consists of basement gneisses, younger granitoids and the Bhima Group of sediments (Fig. 1). It is the NW extension of the Hutti-Maski Schist Belt, comprising of Mesoarchean to Neoarchean volcano-sedimentary sequences (~2.70 – 2.58 Ga) intruded by syn- to late- tectonic granitoids between ~2.62 and 2.55 Ga (Nutman et al., 1996; Chadwick et al., 2000; Jayananda et al., 2006; Sarma et al., 2008). The well foliated basement gneiss occupies the low lying, flat and peneplain topography of the area and contains a linear belt of metabasics (amphibolite/hornblende schist) and scanty acidic volcanic rocks, which are considered equivalent to the Sargur Group. The entire schist belt is about 16 km long and 3 km wide, striking NNW-SSE, and has undergone three phases of deformation and shows green schist to amphibolite facies metamorphism (Ugarkar

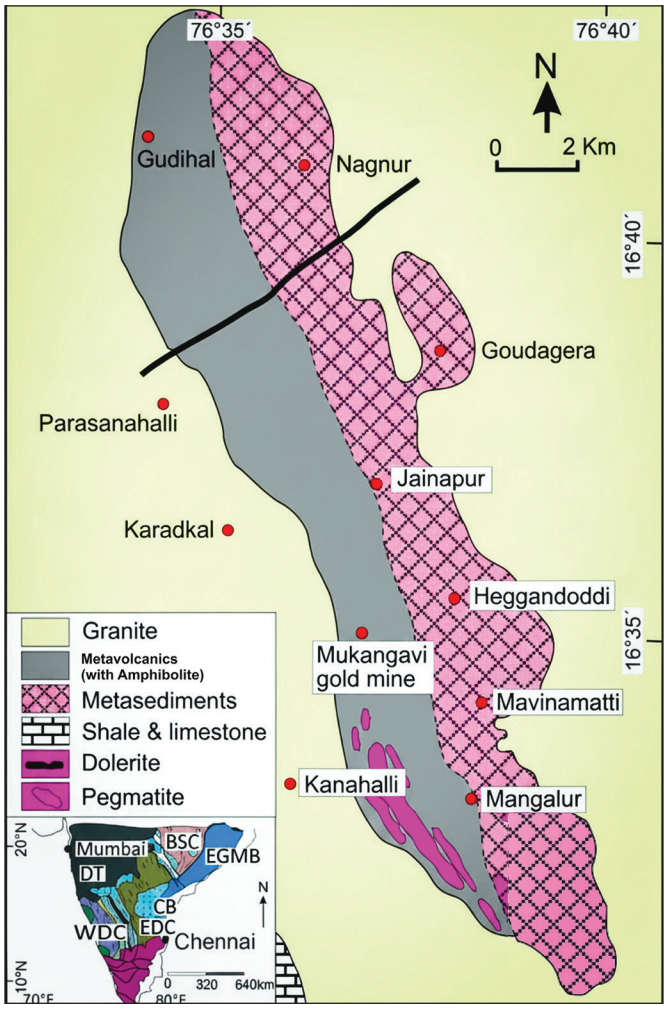


Fig. 1. Geological map of Mangalur Schist Belt, Eastern Dharwar Craton, India (Tenginkai and Ugarkar, 1987).

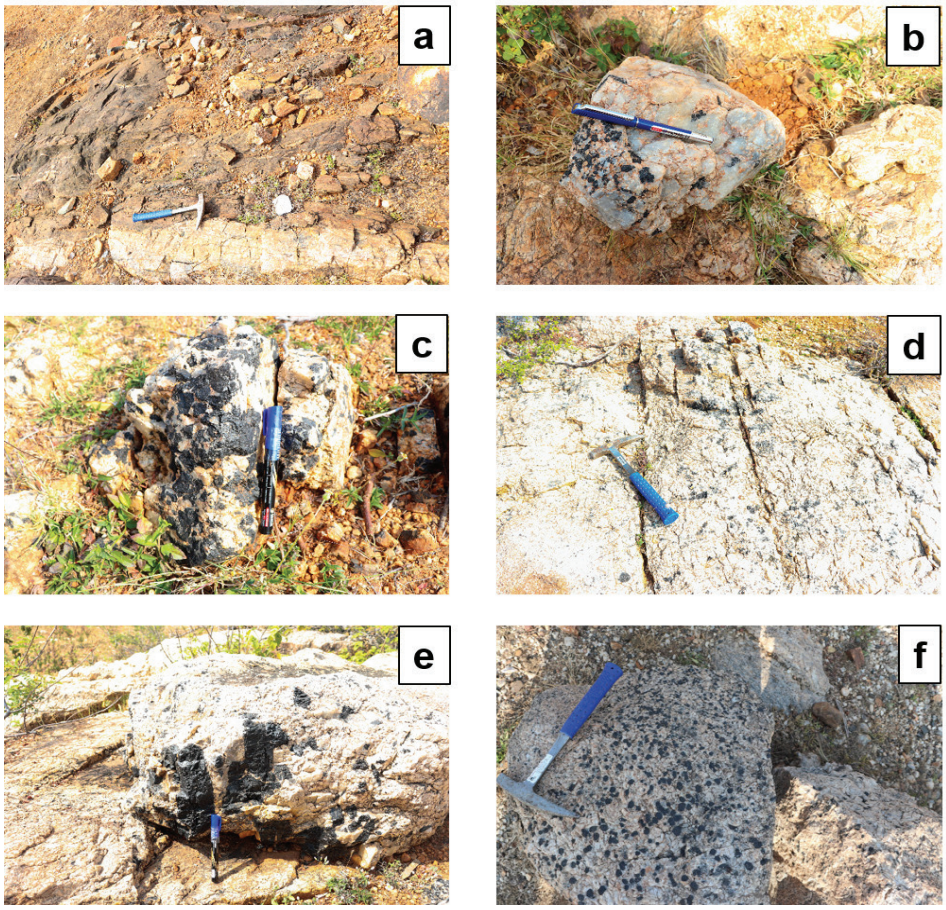


Fig. 2. Field photographs of lithium bearing pegmatite from Mangalur Schist Belt showing (**a**) pegmatite within amphibolite, (**b**) tourmaline bearing pegmatite, (**c**) tourmaline phenocryst in pegmatite, (**d**) tabular body of pegmatite, (**e**) tourmaline megacryst in pegmatite, and (**f**) disseminated tourmaline in pegmatite.

and Tenginkai, 1988, 1989). The younger granites, mostly pink in colour (equivalent to the Closepet granite) (Radhakrishna and Vaidyanadhan, 1997), occur along the southern part of the western margin of the MSB and isolated exposures towards the eastern side of the schist belt. Pegmatites occur as intrusions into the amphibolite and are mostly confined close to the western margin between the schist belt and the Peninsular Gneiss (Fig. 2 a-f).

Field Relationship

Mangalur schist belt is N-S elongated feature enclosed by granite gneiss and younger granitic intrusions. The terrain is predominantly a gently undulating peneplain, with N-S trending amphibolite forming discontinuous linear strike ridges surrounded by extensive granite–gneiss exposures (Fig. 1). Amphibolite is the dominant lithology and is exposed mainly south of Mangalur, southeast of Kanahalli, and west of Ammapur. It is dark grey to black, fine to medium-grained, and occurs as both massive and schistose varieties forming relatively homogeneous, concordant to sub-concordant bands and lensoidal bodies, with foliated and locally discontinuous bands conformable with the regional structural fabric. These bands are composed predominantly of hornblende, epidote, and quartz, with subordinate biotite and garnet, particularly along the eastern margin of the schist belt. Locally, the amphibolite is banded and migmatitic, exhibiting compositional layering, minor folds, and weakly developed migmatitic structures, whereas massive varieties locally preserve vesicular textures. Thin quartz veins transect the amphibolite at several locations, indicating late-stage brittle fracturing and hydrothermal fluid activity.

Pegmatitic and quartzo-feldspathic veins intrude the amphibolite and constitute the youngest intrusion within the schist belt. These bodies are well exposed south of Mangalur, southeast of Kanahalli, and west of Ammapur, where they occur as linear, lensoidal, and tabular bodies emplaced parallel to the regional foliation of the host amphibolite. Individual pegmatite bodies range from approximately 10 to 100 m in length and 5 to 10 m in width, with a predominant NE–SW trend. In the southern part of the study area, spodumene and petalite-bearing pegmatites extend over a strike length of nearly 1 km and attain width upto 5m, suggesting structural control on pegmatite emplacement along pre-existing foliation planes and fracture zones.

The regional structural framework is defined by a penetrative foliation in the amphibolite trending predominantly N–S to NNW–SSE. The schist belt exhibits an overall N–S to NNW–SSE strike, with moderate to steep dips towards both the east and west. Locally, foliation trends NW-SE with westward dips ranging from 50° to 75°.

Secondary structures, including joints, minor folds, and shear-related fabrics, are commonly developed and locally influence the trend of pegmatites.

The surrounding granites are grey to pink, medium- to coarse-grained, and predominantly massive. Along the eastern margin of the schist belt, the amphibolite is intruded by pegmatoidal granite that locally grades into coarse-grained pegmatite. These granitic bodies comprise quartz, K-feldspar, plagioclase, biotite, muscovite, tourmaline, and garnet, and represent evolved felsic magmatism genetically associated with the lithium-bearing pegmatites.

Background and Motivation

Reconnaissance investigations carried out by Atomic Minerals Directorate (AMD) for Exploration and Research, led to the discovery of several rare-metal-bearing pegmatites hosted within the hornblende schists of the Mangalur Schist Belt (MSB) (Thillairaj, 2022). These pegmatites are predominantly distributed south of the Kanahalli–Mangalur road, close to the western contact between the Archean schist sequence and younger intrusive granites. They occur as complex, internally zoned, sub-parallel bodies trending NW–SE and are traceable discontinuously for approximately 3 km. Individual bodies vary considerably in thickness and geometry, reflecting emplacement within structurally controlled fracture systems. The pegmatites host economically significant critical-metal minerals, including spodumene, petalite, and, less commonly, beryl and eucryptite. Visible spodumene crystals bearing pegmatites locally exceed ~1 m in length, indicating favourable conditions for prolonged crystal growth during the late stages of pegmatite evolution. Chemical analyses revealed high Li_2O contents in spodumene and petalite. About fifty pegmatite and spodumene-bearing pegmatite samples were analysed with Li_2O contents ranging from 0.001 to 5.450 wt.% (average 0.598 wt.%) (Thillairaj, 2022). The broad variation in Li_2O reflects heterogeneous spodumene distribution and progressive magmatic differentiation within the pegmatite bodies.

In addition, bulk soil sampling and heavy-mineral concentrate studies by AMD, identified anomalous concentrations of Nb_2O_5 and Ta_2O_5, while X-ray diffraction analyses confirmed the presence of columbite–tantalite. Collectively, the zoned and compositionally evolved nature of the pegmatites, their emplacement within the Archean volcano-sedimentary sequence of the Sargur Group, their close spatial association with younger granitic intrusions, and the occurrence of spodumene, petalite, columbite–tantalite, and beryl indicate a fertile rare-element pegmatite system with significant potential for Li–Cs–Ta (LCT)-type mineralization. Such spodumene-bearing pegmatites are also reported from similar geological setting from the Chhotanagpur Granite Gneiss Complex, Garhtara–Dhangaon area, Korba district, Chhattisgarh (Thillairaj et al., 2024).

METHODOLOGY

A total of fifteen representative, relatively fresh to least-weathered lithium-bearing pegmatite, samples hosted within amphibolites were collected from the Mangalur–Kanahalli area in the southern part of the Mangalur Schist Belt (MSB). The pegmatites are pale white to light green in colour, coarse-grained, and occur as tabular to lens-shaped bodies. These are composed predominantly of quartz, plagioclase, K-feldspar, mica, and spodumene. Each sample was systematically studied for integrated petrographic, mineral chemical, and whole-rock geochemical investigations. Representative splits from the same hand specimen were prepared for thin-section petrography, SEM–EDS mineral chemistry, and whole-rock trace and rare earth element (REE) analyses to ensure direct correlation between mineralogical and geochemical characteristics.

Trace Elements by HR-ICP-MS

Trace elements, including rare earth (REE) and high field strength elements (HFSE), were determined from solutions prepared by dissolving homogenized pegmatite sample powder in a reagent-grade HF:HNO_3 acid mixture in Savillex® screw-top teflon vials. Small portion (0.05 g) of the sample was added to 25 ml teflon pressure decomposition vial, followed by the addition of 10 ml of an acid mixture containing 7:3 HF-HNO_3 to each sample. Subsequently, 5 ml of a 1 ng/ml ^{103}Rh solution was added as an internal standard to each vial. After thorough swirling, the vessels were tightly closed and placed on a hot plate at approximately 140°C for 48 hours. Following this, the vials were opened, and the contents were evaporated at 200°C to near dryness with a few drops of $HClO_4$ to ensure complete removal of HF from the mixture. The residue was further dissolved by adding 10 ml of 1:1 HNO_3, and the volume was adjusted to 250 ml with Milli Q® de-ionized water (18 MΩ). The solution was finally stored in HDPE bottles. Matrix-matching certified reference materials (CRM) JG-1a, JG-2 (GSJ, Japan), GSR-4 (IGGE, China) and G-2 (USGS, USA) along with a couple of procedural blanks, were also prepared using the same protocol described above to minimize errors due to reagents and handling. Clear solutions were obtained for all the samples and calibration standards. These were analyzed at CSIR-NGRI, Hyderabad, using a high-resolution inductively coupled mass spectrometer (HR-ICP-MS) (Nu Instruments Attom®, UK) in peak scan mode at a moderate resolution of 300, which allows accurate measurement of all the analytes of interest (Satyanarayanan et al., 2018). Analytical precision and accuracy were determined from repeated analysis of CRMs and replicate samples. Most of the trace elements exhibited analytical precision better than 5% relative standard deviation (RSD), and the measured concentrations were in good agreement with the certified values (Table 1).

SEM-EDS Analysis

Mineralogical data from typical samples were acquired at CSIR-NGRI, Hyderabad, using Scanning Electron Microscope (Hitachi®) equipped with an Energy Dispersive Spectrometer (SEM-EDS) for semi-quantitative chemical analysis. The minerals were investigated using reflected light and scanning electron microscopy, and back-scattered images (BSE) were acquired. Chemical compositions were determined using the Oxford Inca® energy dispersive analytical system (EDS), operating at accelerating voltage of 15 kV, beam current of 2.9 nA and measurement time of 60 seconds. Atomic ratios were calculated with the ZAF-4® program, which performs the necessary corrections for the overlapping peaks of different elements.

Table 1. Analytical data, standard deviations (SD) of certified reference materials (CRM) JG-1A (GSJ, Japan), G-2 (USGS) and AC-E (ANRT, France) obtained by HR-ICP-MS in the present study and reported value from Govindaraju (1994) and GEOREM (georem.mpch-mainz.gwdg.de)

Analyte	Mass No.	JG-1A				G-2				AC-E			
		A	B	SD	%RSD	A	B	SD	%RSD	A	B	SD	%RSD
Li	7	81.939	85.900	3.200	3.758	34.354	33.800	2.368	6.891	89.783	93.000	0.360	0.401
Sc	45	6.420	6.310	0.417	6.262	3.550	3.580	0.031	0.881	0.118	0.110	0.003	2.380
V	51	23.287	23.000	0.209	0.888	35.292	35.560	0.486	1.378	3.638	3.000	0.321	8.822
Cr	52	19.621	18.600	0.536	2.712	8.630	8.290	0.185	2.148	3.760	3.400	0.229	6.082
Co	59	5.392	5.700	0.210	4.008	4.908	4.539	0.088	1.800	0.234	0.200	0.009	3.958
Ni	60	6.068	6.400	0.116	1.948	4.720	4.230	0.049	1.032	1.489	1.500	0.024	1.579
Cu	63	1.272	1.300	0.004	0.342	10.738	10.990	0.720	6.705	4.444	4.000	0.052	1.163
Zn	66	38.911	38.800	0.523	1.340	85.347	84.250	6.429	7.533	251.795	224.000	21.516	8.545
Ga	71	16.774	17.000	0.415	2.442	23.272	23.160	0.050	0.217	42.383	39.000	0.980	2.313
Rb	85	178.320	180.000	11.289	6.709	152.716	169.250	1.397	0.914	136.666	152.000	4.336	3.173
Sr	88	179.302	185.000	1.934	1.087	473.567	476.450	1.671	0.353	3.541	3.000	0.052	1.459
Y	89	30.934	31.600	0.799	2.645	11.980	10.440	0.129	1.074	215.766	184.000	9.825	4.554
Zr	90	117.677	121.000	3.070	2.672	262.120	314.000	4.774	1.821	739.992	780.000	27.793	3.756
Nb	93	11.578	12.000	0.237	2.088	13.007	12.010	0.264	2.029	115.807	110.000	2.016	1.740
Cs	133	11.110	11.400	0.063	0.573	1.401	1.349	0.005	0.357	2.884	3.000	0.030	1.045
Ba	137	445.386	458.000	2.882	0.652	1884.708	1866.000	18.254	0.969	57.076	55.000	3.476	6.089
La	139	21.301	21.800	0.103	0.488	99.346	88.700	0.495	0.498	63.987	59.000	1.632	2.551
Ce	140	44.307	45.200	0.368	0.841	177.613	160.600	2.663	1.499	165.859	154.000	3.876	2.337
Pr	141	5.962	6.080	0.036	0.617	20.934	17.440	0.115	0.550	26.068	22.200	1.211	4.647
Nd	146	20.589	21.000	0.109	0.535	61.251	54.405	0.422	0.688	102.001	92.000	3.191	3.128
Sm	147	4.734	4.850	0.034	0.724	8.080	7.195	0.047	0.578	26.966	24.200	0.886	3.285
Eu	151	0.709	0.720	0.008	1.147	1.252	1.407	0.014	1.089	1.790	2.000	0.058	3.241
Gd	157	3.710	3.750	0.045	1.220	3.721	4.265	0.029	0.789	23.514	26.000	0.670	2.851
Tb	159	0.779	0.790	0.009	1.202	0.505	0.488	0.009	1.775	5.006	4.800	0.080	1.599
Dy	163	4.094	4.200	0.052	1.287	1.978	2.339	0.001	0.061	27.470	29.000	0.358	1.302
Ho	165	0.736	0.760	0.009	1.226	0.382	0.386	0.006	1.543	5.595	6.500	0.238	4.245
Er	166	2.333	2.360	0.036	1.583	0.976	0.924	0.001	0.099	15.781	17.700	0.501	3.173
Tm	169	0.377	0.390	0.002	0.479	0.155	0.152	0.001	0.351	2.495	2.600	0.020	0.798
Yb	172	2.667	2.740	0.039	1.481	0.646	0.761	0.000	0.073	16.947	17.400	0.097	0.570
Lu	175	0.438	0.440	0.006	1.359	0.093	0.106	0.000	0.369	2.563	2.450	0.039	1.527
Hf	178	3.822	3.840	0.051	1.334	7.119	7.840	0.042	0.590	27.921	27.900	1.882	6.741
Ta	181	1.694	1.700	0.010	0.573	0.644	0.690	0.000	0.023	5.621	6.400	0.231	4.107
Pb	208	26.411	27.000	0.392	1.490	29.644	30.000	0.045	0.153	34.502	39.000	3.573	10.355
Th	232	11.797	12.100	0.227	1.933	22.728	24.770	0.197	0.866	16.983	18.500	0.371	2.184
U	238	4.605	4.700	0.138	3.013	1.727	2.017	0.011	0.630	4.446	4.600	0.022	0.501

A – Value from HR-ICP-MS (average of 6)
B – Value from Govindaraju (1994) and GEOREM (georem.mpch-mainz.gwdg.de)

RESULTS

Petrography and Mineral Chemistry

Mangalur pegmatites display a holocrystalline, coarse-grained, typically inequigranular texture that shows transitions locally into graphic intergrowths characterized by quartz, feldspar and mica reflecting late-stage fluid activity. The primary mineral texture is dominated by quartz, plagioclase, K-feldspar, and biotite, with distinct inter-granular association (Fig. 3 a-f).

Quartz: Occurs as large, anhedral grains displaying undulose extinction and sub-grain boundary development under cross-polarized light. This indicates that the pegmatite bodies experienced post-crystallization strain during Neoarchean deformation. In highly fractionated domains, quartz forms fine-grained granular aggregates flanking larger feldspar phenocrysts.

Plagioclase and K-Feldspar: Plagioclase manifests as subhedral laths exhibiting well-defined albite polysynthetic twinning.

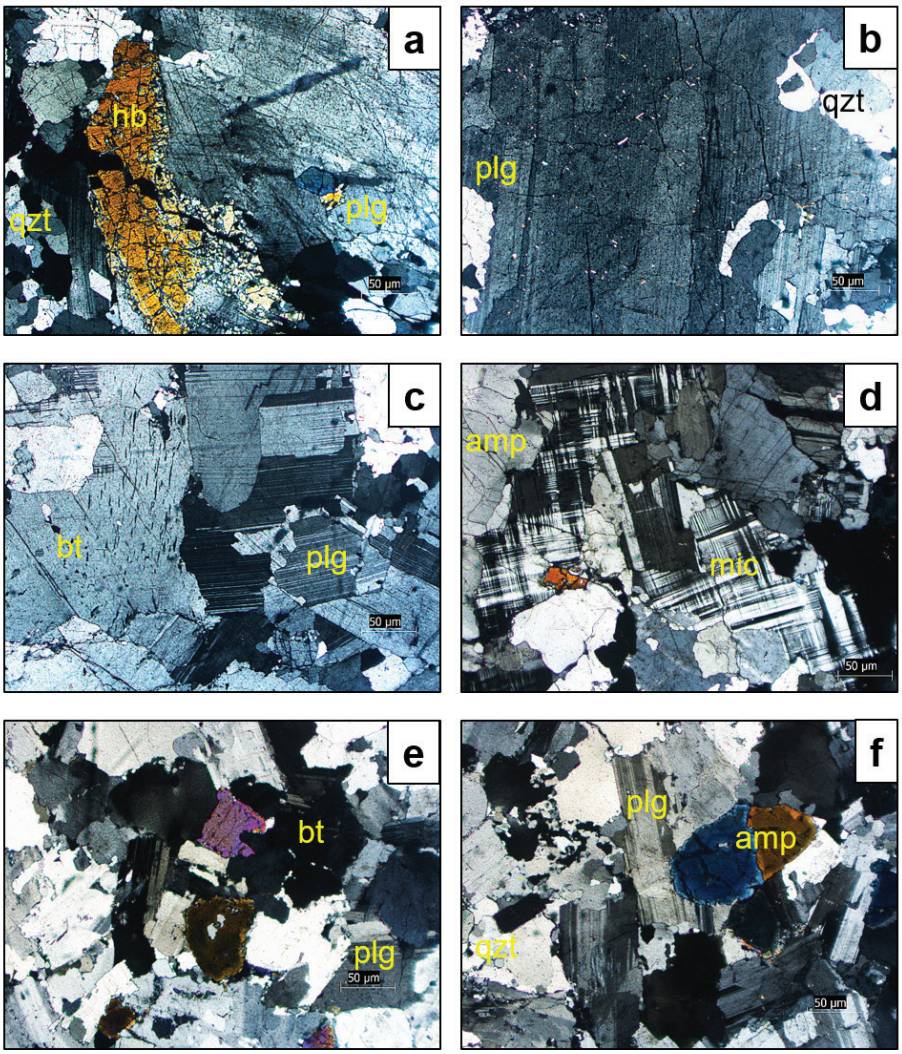


Fig. 3(a-f). Thin section photographs of pegmatite from Kanahalli-Mangalur section, Mangalur Schist Belt showing various minerals.

K-feldspar appears as microcline showing characteristic cross-hatched (tartan) twinning, as well as untwinned orthoclase. Locally, graphic intergrowths between quartz and K-feldspar are widespread, representing simultaneous eutectic crystallization from a highly evolved, volatile-saturated residual melt.

Biotite and secondary alteration: Biotite occurs as elongated primary grains with volatile-driven hydrothermal alteration, that has partially to almost completely transformed these primary micas into chlorite. This chloritization is accompanied by the exsolution of iron oxides along cleavage planes, indicating late-stage magmatic-hydrothermal overprinting.

SEM-BSE and EDS Microanalysis

SEM-EDS microanalyses further indicate the mineral chemistry and crystallization sequences, specifically targeting accessory phases critical to understanding the volatile budget. SEM-EDS data indicate the presence of primary fluorapatite hosted within the feldspathic and quartz matrix (Fig. 4 a-c). They appear as bright, high-relief subhedral to anhedral crystals trapped within the interstitial spaces between K-feldspar and quartz. The presence of primary fluorapatite suggests that the parental melt was enriched in phosphorus and halogens as fluxing agents, and these elements are known to dramatically lower the solidus temperature of granitic melts, reduce viscosity, and significantly prolong the fractional crystallization process (Baker and Vaillancourt, 1995; Bartels et al., 2013). This allowed elements such as lithium, which could not get accommodated in early formed major silicates, concentrated in the residual liquid. The evolutionary sequence can be deduced as (i) early magmatic crystallization of quartz, feldspars, and biotite, followed by (ii) accumulation of volatiles and P–F-rich components that lower the melt solidus, and (iii) a late hydrothermal stage characterized by fluorapatite precipitation and chloritization.

GEOCHEMISTRY

Trace Element and REE Characteristics

The trace and rare-earth elements (REE) in pegmatites from the Mangalur Schist Belt (MSB) (Table 2) exhibit variations with

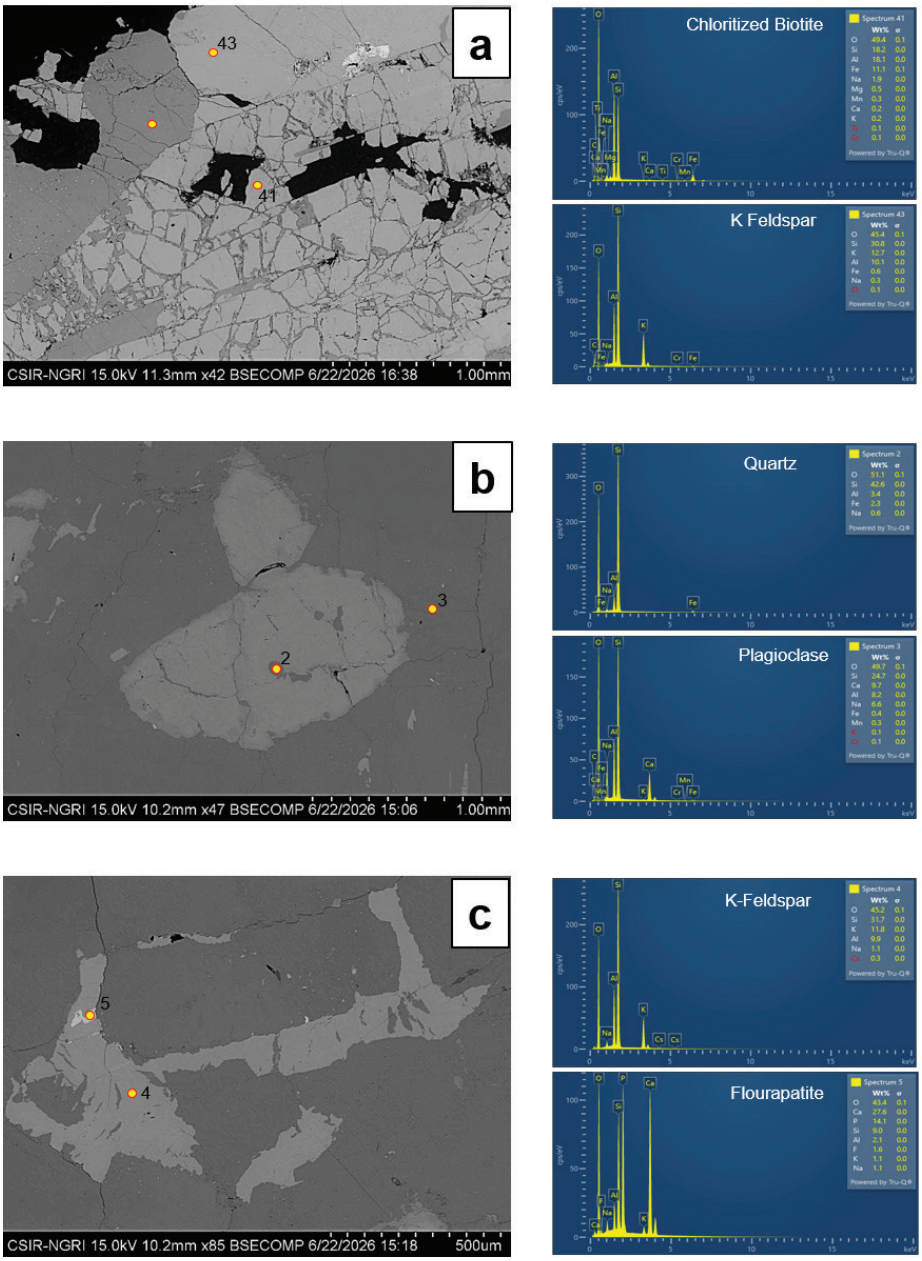


Fig. 4 (a-c). BSE image and EDS spectra of lithium bearing pegmatite from Mangalur Schist Belt.

a highly fractionated REE signature (Fig. 5) and multi-element patterns (Fig. 6) characteristic of granitic systems. The geochemical behavior of incompatible trace elements reveals progressive differentiation pathways within the pegmatite suite. Among rare alkalis, lithium concentrations demonstrate substantial enrichment variations, ranging from background baseline values of 6.5 ppm in sample MG-10 to an elevated peak of 97.3 ppm in sample MG-18. This pronounced enrichment profile is closely followed by rubidium and caesium. Selected spodumene-bearing pegmatite samples were hand-picked to isolate grains identified as spodumene for chemical analysis. These grains contain approximately 5.6–6.1 wt.% Li, corresponding to calculated Li_2O contents of approximately 12.1–13.1 wt.%, consistent with the composition of spodumene. Rubidium displays extreme concentration spikes, reaching up to 1275.5 ppm (MG-10) and 1698.5 ppm (MG-11). Similarly, Caesium concentrations systematically increase up to 117.9 ppm (MG-10) and 119.00 ppm (MG-19), establishing a clear link to an LCT (Lithium-Cesium-Tantalum) pegmatites. High-Field Strength Elements (Nb, Ta, Zr, Hf) show significant enrichment trends across specific sample sets. Niobium reaches up to 150.3 ppm in sample MG-11 and 111.0 ppm in sample MG-13, while tantalum displays peak values of 26.2 ppm (MG-11) and 42.6 ppm (MG-13). Zirconium contents remain moderately restricted between 24.0 ppm and 73.8 ppm, coupled with narrow hafnium concentrations of 0.9 ppm to 4.7 ppm, supporting a highly evolved crustal status. Among compatible and alkaline earth elements, strontium concentrations are heavily depleted across

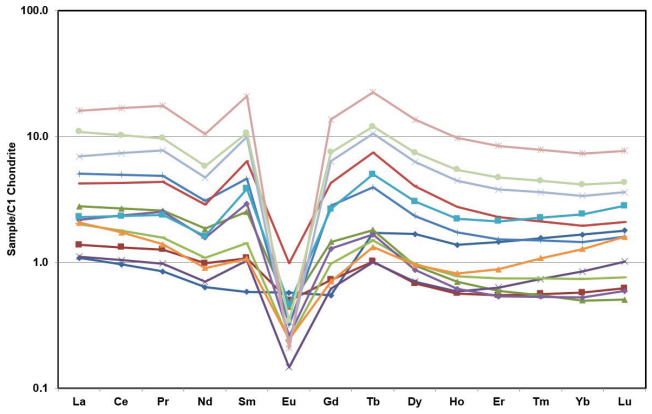


Fig. 5. Chondrite normalized REE pattern of lithium bearing pegmatite.

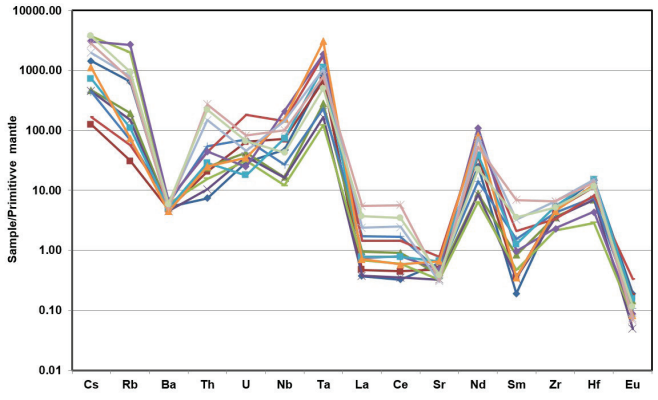


Fig. 6. Primitive mantle normalized multi-element diagram of lithium bearing pegmatite.

the entire suite, strictly constrained within a narrow window of 6.4 ppm to 16.5 ppm. Barium behaves similarly, ranging only from 31.2 ppm to 48.3 ppm. This pronounced depletion of Sr and Ba serves as a clear geochemical indicator of extensive, earlier fractional crystallization of plagioclase and K-feldspar before injection of the final residual liquid (McCaffrey and Jowitt, 2023). The total rare earth element (ΣREE) concentrations of the Mangalur pegmatites are uniformly low, with all samples exhibiting exceptionally depleted REE abundances relative to typical granitic pegmatites. Lanthanum ranges from 0.26 ppm to 3.76 ppm, and Cerium between 0.58 ppm and 10.1 ppm. HREE concentrations are similarly low, with ytterbium values between 0.08 ppm and 1.2 ppm. The uniformly low ΣREE contents are characteristic of highly evolved pegmatitic melts, reflecting extensive fractionation during magmatic evolution (Breiter et al., 2023). The depletion of REEs is commonly attributed to their early sequestration into accessory minerals such as monazite, xenotime, zircon, and allanite during granite differentiation, resulting in a residual melt depleted in REEs prior to pegmatite emplacement.

Differentiation Ratios and Fractionation Indices

To quantify the degree of magmatic evolution and elucidate the fractional crystallization sequence of the Mangalur pegmatites, few geochemical fractionation indices (K/Rb, Nb/Ta, and Zr/Hf) were calculated from the whole-rock dataset. The systematic decrease in these elemental ratios reflects progressive magmatic differentiation and the evolution of increasingly fractionated residual melts. Low K/Rb ratios record extensive K-feldspar fractionation accompanied by progressive enrichment of Rb in the residual melt. Likewise, decreasing Nb/Ta ratios (~2.6) indicate advanced fractionation of Nb–Ta-bearing oxide minerals, resulting in preferential enrichment of Ta in the late-stage, in F-bearing residual melts. The concurrent decline in Zr/Hf ratios (~15.7) reflects increasing fractionation of high-field-strength elements (HFSEs) during late-stage magmatic evolution (Zozulya et al., 2022). Collectively, these geochemical trends indicate relatively intense fractionation and rare-element enrichment in LCT pegmatite systems (Morozova et al., 2022; Kaeter et al., 2023; McCaffrey and Jowitt, 2023).

DISCUSSION

The integration of petrographic observations with whole-rock geochemistry indicates that lithium enrichment in the Mangalur Schist Belt pegmatites resulted from the combined effects of prolonged magmatic differentiation and volatile-assisted evolution of a residual granitic melt. The systematic enrichment of Li (up to 97.3 ppm) with spodumene bearing samples showing very high concentration of up to 6.1 wt.%, Rb (up to 1698 ppm), and Cs (up to 119 ppm), coupled with pronounced depletion of Sr and Ba and progressively decreasing K/Rb, Nb/Ta, and Zr/Hf ratios, records an advanced stage of pegmatite evolution through prolonged fractional crystallization. These geochemical characteristics are consistent with derivation from a highly evolved, peraluminous S-type granitic magma through progressive fractional crystallization, rather than direct anataxis of a local metamorphic source (Chakraborty and Upadhyay, 2020). Sequential crystallization and removal of plagioclase, K-feldspar, biotite, and Nb-bearing oxide phases progressively depleted the melt in compatible elements while concentrating incompatible components, including Li, Rb, Cs, Ta, and other rare metals, within the residual liquid. Such fractionation trends are widely regarded as diagnostic features of evolved LCT pegmatite systems (Kaeter et al., 2023; McCaffrey and Jowitt, 2023).

Petrographic evidence further demonstrates that volatile enrichment exerted a fundamental control on the physicochemical evolution of the pegmatitic melt. The presence of primary fluorapatite as an early magmatic accessory phase indicates elevated fluorine and phosphorus concentrations in the parental melt, characteristic of highly evolved granitic systems. Fluorine is known to depolymerize silicate melts by disrupting Si–O–Si linkages, thereby reducing melt viscosity, depressing the solidus temperature, and significantly enhancing melt mobility. Experimental investigations further demonstrate that F-rich granitic melts remain liquid over a broader temperature interval, promoting prolonged crystallization and continued chemical differentiation (Baker and Vaillancourt, 1995; Bartels et al., 2013). The presence of phosphorus, recorded by fluorapatite crystallization, likewise reflects an evolved melt enriched in incompatible components and contributes to the stabilization of late-stage accessory mineral assemblages.

Table 2. Trace and REE data (in ppm) of lithium bearing pegmatites from the Mangalur Schist Belt, Eastern Dharwar Craton.

Analyte	MG-1	MG-2	MG-3	MG-4	MG-8	MG-9	MG-10	MG-11	MG-12	MG-13	MG-16	MG-18	MG-19
Li	12.0	26.5	38.9	8.1	14.7	10.9	6.5	9.5	19.0	73.9	71.6	97.3	39.7
Sc	7.8	5.0	8.5	0.9	1.0	9.1	0.5	3.6	7.4	9.8	6.4	6.8	4.3
V	3.9	16.4	18.7	2.8	3.0	6.8	4.1	2.8	2.7	4.5	5.1	2.6	4.8
Cr	19.8	25.1	103.1	20.4	16.4	14.9	23.9	22.1	17.0	24.7	23.5	23.0	48.2
Co	1.1	2.8	6.8	0.6	0.8	2.2	1.5	1.0	1.6	1.4	1.1	0.9	1.7
Ni	12.3	19.2	74.8	14.0	11.0	14.4	16.1	15.6	12.9	19.1	11.9	16.0	31.4
Cu	1.4	1.4	1.9	1.2	1.3	2.8	1.4	2.9	1.6	1.9	1.3	1.4	1.6
Zn	18.9	72.3	124.8	24.0	22.4	107.8	40.7	56.0	51.1	115.3	90.5	88.9	62.2
Ga	43.8	23.3	44.8	11.2	26.6	51.6	22.4	35.6	52.2	68.3	40.0	39.7	35.7
Rb	416.1	19.8	124.7	94.2	43.9	36.0	1275.5	1698.5	70.2	46.7	502.0	451.0	599.0
Sr	13.0	10.1	8.3	6.8	9.4	16.5	6.8	10.1	13.8	13.8	6.4	6.9	8.3
Y	5.3	3.6	3.7	3.4	5.6	7.6	3.8	3.1	7.0	3.9	11.3	21.6	14.0
Zr	54.6	52.7	40.4	39.0	47.4	37.2	24.0	26.0	60.3	50.2	73.8	73.0	58.2
Nb	33.8	51.0	11.8	11.5	19.3	103.0	8.6	150.3	52.3	111.0	101.8	71.7	30.2
Mo	2.2	3.3	14.9	2.6	2.3	3.0	3.2	3.1	2.0	4.0	2.1	3.4	5.6
Cs	45.8	4.0	15.0	14.3	14.0	5.3	117.9	97.8	23.4	35.5	62.9	89.9	119.0
Ba	36.8	33.7	35.6	31.5	42.2	48.3	42.0	46.6	35.6	31.2	39.3	34.5	41.7
La	0.26	0.32	0.66	0.26	1.19	0.99	0.47	0.51	0.54	0.49	1.64	3.76	2.55
Ce	0.58	0.79	1.62	0.63	2.99	2.58	1.08	1.41	1.40	1.04	4.43	10.10	6.19
Pr	0.08	0.11	0.23	0.09	0.43	0.39	0.14	0.22	0.21	0.12	0.69	1.56	0.86
Nd	0.29	0.44	0.84	0.32	1.39	1.30	0.49	0.71	0.73	0.41	2.13	4.71	2.63
Sm	0.09	0.16	0.37	0.15	0.68	0.94	0.21	0.43	0.56	0.16	1.45	3.06	1.57
Eu	0.03	0.03	0.02	0.01	0.02	0.06	0.01	0.01	0.03	0.01	0.01	0.01	0.02
Gd	0.11	0.14	0.29	0.12	0.55	0.84	0.19	0.25	0.52	0.14	1.25	2.68	1.47
Tb	0.06	0.04	0.07	0.04	0.14	0.27	0.05	0.06	0.18	0.05	0.38	0.80	0.43
Dy	0.41	0.17	0.23	0.17	0.57	0.98	0.24	0.21	0.74	0.23	1.52	3.30	1.80
Ho	0.08	0.03	0.04	0.03	0.10	0.15	0.04	0.03	0.12	0.05	0.25	0.55	0.30
Er	0.23	0.09	0.09	0.10	0.24	0.36	0.12	0.09	0.34	0.14	0.60	1.33	0.75
Tm	0.04	0.01	0.01	0.02	0.04	0.05	0.02	0.01	0.05	0.03	0.09	0.19	0.11
Yb	0.27	0.09	0.08	0.14	0.24	0.32	0.12	0.09	0.39	0.21	0.55	1.20	0.68
Lu	0.04	0.02	0.01	0.02	0.04	0.05	0.02	0.01	0.07	0.04	0.09	0.18	0.10
Hf	4.58	3.55	2.13	2.18	2.38	2.52	0.89	1.36	4.66	3.88	4.70	4.16	3.55
Ta	11.43	9.31	3.89	2.33	3.26	24.78	1.70	26.21	15.86	42.66	14.78	11.24	6.94
Pb	8.39	9.91	7.25	7.87	8.40	12.82	17.54	11.39	8.28	7.43	10.74	11.11	12.91
Th	0.63	1.75	2.08	0.89	4.63	3.72	1.32	3.81	2.45	2.12	12.65	22.95	18.93

The combined effects of prolonged fractional crystallization and volatile enrichment progressively transformed the parental S-type granitic magma into an increasingly evolved residual melt enriched in Li, Rb, Cs, Ta and other incompatible elements. In the LCT pegmatite system, this evolutionary trend is expressed by the progressive development of rare-metal mineral assemblages, commonly ranging from beryl- and columbite-bearing assemblages in relatively less evolved domains to columbite–tantalite- and spodumene-bearing assemblages in more highly fractionated domains (Černý and Ercit, 2005; Černý et al., 2012). The preferential retention of Li, Rb and Cs in the residual melt, coupled with progressive Nb–Ta fractionation, promoted the development of Li-rich residual liquids. Enrichment in volatile components, particularly F and P, further modified the physicochemical properties of the residual melt, enhancing its mobility and facilitating its migration into structurally favourable sites within the Mangalur Schist Belt. Continued differentiation of these volatile-rich residual melts ultimately produced the rare-metal mineral assemblages characteristic of highly evolved LCT pegmatites, including spodumene and associated Ta-bearing phases. The Mangalur pegmatites are therefore interpreted as products of advanced fractional crystallization of a fertile, peraluminous S-type granitic magma, with volatile-assisted differentiation playing an important role in the concentration and late-stage emplacement of Li and other rare metals. This model is consistent with the established

petrogenetic relationship between LCT pegmatites and S-type granites and with the progressive mineralogical and geochemical evolution recognized in rare-element pegmatite systems worldwide (Černý and Ercit, 2005; Černý et al., 2012).

Comparison between Mangalur and Amareshwar Pegmatites

The Mangalur pegmatite body is widely regarded as an extension of the Amareshwar pegmatites, where lithium-bearing pegmatites have been extensively documented and confirmed by several studies. Furthermore, the Hutti Schist Belt extends northward and encloses the Mangalur Schist Belt, as reported by Rao (1980). A comparison of the Mangalur and Amareshwar pegmatites reveals notable mineralogical differences (Fig. 7). SEM–EDS analyses indicate that the Mangalur pegmatites lack zinnwaldite. In contrast, the mineral has been reported from the Amareshwar pegmatites (Sindhuja et al., 2025). In addition, the two pegmatite bodies differ in their modal mineralogical compositions. These variations can be attributed to differences in the degree of magmatic fractionation during fractional crystallization, as well as the influence of volatile- and flux-rich granitic melts (Singh et al., 2026).

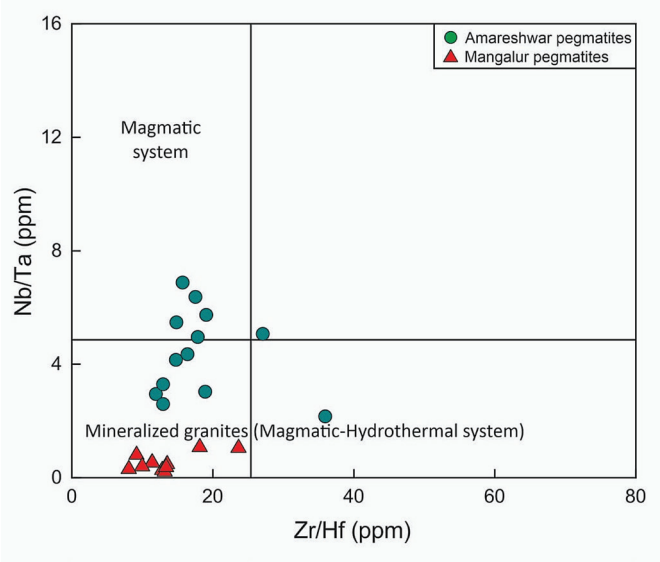


Fig. 7. Bivariate diagram of Zr/Hf vs Nb/Ta (after Pfänder et al., 2007) showing Mangalur and Amareshwar pegmatites plots in different fields of mineralized granites of magmatic-hydrothermal origin.

CONCLUSIONS

Integrated petrographic, mineral chemical, and whole-rock geochemical investigations indicate that the Mangalur Schist Belt pegmatites represent an evolved rare-element pegmatite system formed through magmatic differentiation. Petrographic evidence, including graphic quartz–feldspar intergrowths and primary fluorapatite, together with whole-rock geochemistry, suggests crystallization from a volatile-rich residual granitic melt. Systematic enrichment of Li, Rb, and Cs, coupled with depletion of Sr and Ba and progressively decreasing K/Rb, Nb/Ta, and Zr/Hf ratios, records extensive fractional crystallization and enrichment of incompatible elements during melt evolution. The occurrence of fluorapatite further indicates presence of fluorine- and phosphorus-bearing volatiles, which likely reduced melt viscosity and depressed the solidus temperature, thereby prolonging crystallization and enhancing the enrichment of rare elements in the residual melt. Although the whole-rock lithium concentrations are modest with spodumene bearing samples showing as high as 6.1 wt.%, the combined mineralogical and geochemical signatures demonstrate that the Mangalur pegmatites possess the characteristic evolutionary features of fertile LCT-type pegmatite systems. This study provides the first comprehensive genetic framework for the Mangalur pegmatites and identifies the western margin of the Eastern Dharwar Craton as a prospective terrain for critical elements mineralization. These findings provide a scientific basis for future mineral-chemical, isotopic, geochronological, and exploration studies aimed at evaluating the lithium and other critical minerals potential of the region.

Acknowledgement: The authors thank the Director, CSIR–National Geophysical Research Institute (CSIR–NGRI), Hyderabad, for granting permission to publish this work. Financial support from the Council of Scientific and Industrial Research (CSIR), India, through the FBR-050306 project at CSIR–NGRI is gratefully acknowledged. Professor G. Parthasarathy sincerely acknowledges the Department of Atomic Energy (DAE), Government of India, for support under the DAE Raja Ramanna Chair Scheme. The authors are also grateful to Professor Sarada P. Mohanty and Dr. Ashit Kumar Swain of the Geological Survey of India for their kind invitation to contribute this article to the special volume, Natural Resources and Their Utilization with Special Reference to Critical Minerals (NATURE-CM 2026).

References

Baker, D.R., and Vaillancourt, J. (1995) The low viscosities of F + H_2O-bearing granitic melts and implications for melt extraction and transport. Earth and Planetary Science Letters, v.132, pp.199–211.

Balaram, V., Santosh, M., Satyanarayanan, M., Srinivas, N. and Gupta, H. (2024) Lithium: A review of applications, occurrence, exploration, extraction, recycling, analysis, and environmental impact. Geoscience Frontiers, v.15(5), Article 101868.

Bartels, A., Behrens, H., Holtz, F., Schmidt, B.C., Fechtelkord, M., Knipping, J., Crede, L., Baasner, A. and Pukallus, N. (2013) The effect of fluorine, boron and phosphorus on the viscosity of pegmatite-forming melts. Chemical Geology, v.346, pp.184–198.

Breiter, K., Vašinová Galiová, M., Hložková, M., Korbelová, Z., Kynický, J. and Costi, H.T. (2023) Trace element composition of micas from rare-metal granites of different geochemical affiliations. Lithos, v.448–449, Article 107135.

Černý, P. and Ercit, T. S. (2005) The classification of granitic pegmatites revisited. The Canadian Mineralogist, v.43(6), pp.2005–2026.

Černý, P., London, D. and Novák, M. (2012) Granitic pegmatites as reflections of their sources. Elements, v.8(4), pp.289–294.

Chadwick, B., Vasudev, V.N. and Hegde, G.V. (2000) The Dharwar Craton, southern India, interpreted as the result of Late Archaean oblique convergence. Precambrian Research, v.99, pp.91–111.

Chakraborty, T. and Upadhyay, D. (2020) The geochemical differentiation of S-type pegmatites: constraints from major–trace element and Li–B isotopic composition of muscovite and tourmaline. Contributions to Mineralogy and Petrology, v.175, pp.60. https://doi.org/10.1007/s00410-020-01697-x

Curtis, L.C. and Radhakrishna, B.P. (1993) Gadag Gold—A Challenging Prospect. Economic Geology Series No. 3, Geological Society of India, Bangalore, 195p

Devaraju, T.C., Rajashekhar, N., Srikantappa, C., Khanadali, S.D. and Subba Rao, G. (1990) Lithium pegmatites of Amareshwar, Raichur District, Karnataka, India. In: Naqvi, S.M. (Ed.), Precambrian Continental Crust and its Economic Resources. Developments in Precambrian Geology, Elsevier, Amsterdam, v.8, pp. 653–669.

Govindaraju, K. (1994) Compilation of working values and sample description for 383 geostandards. Geostandards Newsletter, v.18, Special Issue no.1, pp.1–158

Greim, P., Solomon, A.A., and Breyer, C. (2020) Assessment of lithium criticality in the global energy transition and addressing policy gaps in transportation. Nature Communications, v.11, Article 4570.

Grosjean, C., Herrera Miranda, P., Perrin, M. and Poggi, P. (2012) Assessment of world lithium resources and consequences of their geographic distribution on the expected development of the electric vehicle industry. Renewable and Sustainable Energy Reviews, v.16(3), pp.1735–1744.

Jayananda, M., Chardon, D., Peucat, J.J. and Capdevila, R. (2006) 2.61 Ga potassic granites and crustal reworking in the Eastern Dharwar Craton, southern India: Tectonic, geochronologic and geochemical constraints. Precambrian Research, v.150, pp.1–26.

Jayananda, M., Peucat, J. J., Chardon, D., Rao, B. K., Fanning, C. M. and Corfu, F. (2013) Neoarchean greenstone volcanism and continental growth, Dharwar Craton, southern India: Constraints from SIMS U–Pb zircon geochronology and Nd isotopes. Precambrian Research, v.227, pp.55–76.

Kaeter, D., Barros, R., Menuge, J.F. and Chew, D.M. (2023) The role of columbite-group minerals in tracing the evolution of rare-element granitic pegmatites. Minerals, v.13(8), Article 1048.

Kesler, S.E., Gruber, P.W., Medina, P.A. and Keoleian, G.A., Everson, M.P. and Wallington, T.J. (2012) Global lithium resources: Relative importance of pegmatite, brine and other deposits. Ore Geology Reviews, v.48, pp.55–69.

Kundu, T., Rath, S.S., Das, S.K., Parhi, P.K. and Angadi, S.I. (2023a) Recovery of lithium from spodumene-bearing pegmatites: A comprehensive review on geological reserves, beneficiation, and extraction. Powder Technology, v.415, Article 118142.

Kundu, T., Rath, S.S., Das, S.K., Parhi, P.K. and Angadi, S.I. (2023b) Characterization and gravity concentration studies on spodumene-bearing pegmatites of India. Separation Science and Technology, v.58(13), pp.2331–2343.

Linnen, R. L., Hanley, J. J. and Dewolfe, J. C. (2012) The links between volatile evolution, Element partitioning, and the mineralization of granitic pegmatites. Transactions of the Royal Society of Edinburgh: Earth Sciences, v.103(1), pp.1–15.

London, D. (2008) Pegmatites. Mineralogical Association of Canada Special Publication, v.10, 347p.

Maneta, V. and Baker, D.R. (2017) Experimental crystallization of undercooled felsic liquids: Generation of pegmatitic texture. Journal of Petrology, v.58(3), pp.539–564.

Manikyamba, C. and Kerrich, R. (2012) Eastern Dharwar Craton, India: Continental lithosphere growth by accretion of diverse plume and arc terranes. Geoscience Frontiers, v.3(3), pp.225–240.

McCaffrey, D., and Jowitt, S.M. (2023) The crystallization temperature of granitic pegmatites: The important relationship between undercooling and critical metal prospectivity. Earth-Science Reviews, v.244, Article 104541.

Morozova, L., Zozulya, D., Selivanova, E., Serov, P. and Bazai, A. (2022) Distribution of trace elements in K-feldspar with implications for tracing ore-forming processes in pegmatites: Examples from the world-class Kolmozero lithium deposit, NW Russia. Minerals, v.12(11), Article 1448.

Naqvi, S.M., Rana Prathap, J.G. and Mohan, M.R. (2008) Role of adakitic magmatism and subduction in gold endowment of Dharwar Neoarchaean greenstone belts, India. Journal of the Geological Society of India, v.72(4), pp.576–577

Nutman, A.P., Chadwick, B., Ramakrishnan, M., and Viswanatha, M.N. (1996) SHRIMP U–Pb zircon ages of granitoids from the Dharwar Craton and implications for Archean crustal evolution. Precambrian Research, v.78, pp.1–24.

Pandey, A. (2025). Lithium: potential and possibilities in the pegmatite belts of India - global perspectives and exploration strategies. International Geology Review, v. 67(5), pp. 649-674.

Peucat, J.-J., Jayananda, M., Chardon, D., Capdevila, R., Fanning, C.M. and Paquette, J.-L. (2013) The lower crust of the Dharwar Craton, southern India: Patchwork of Archean granulitic domains. Precambrian Research, v.227, pp.4–28.

Pfänder, J.A., Münker, C., Stracke, A. and Mezger, K. (2007) Nb/Ta and Zr/Hf in ocean island basalts: Implications for crust–mantle differentiation and the fate of niobium. Earth and Planetary Science Letters, v.254(1–2), pp.158–172.

Radhakrishna, B.P. and Vaidyanadhan, R. (1997) Geology of Karnataka. 2nd revised and enlarged edition. Geological Society of India, Bangalore, xii + 353p.

Rao, M.N.R. (1980) Mangalur Gold Prospect - A case study review. In: Proceedings of the Seminar on Recent Trends in Gold Mining Practice, India. Geological Society of India, Bangalore, pp.1–6.

Saikia, B.J., Parthasarathy, G., Saikia, B.K., Bordoloi, P., Borah, R.R., Srivastava, P.K. and Satyanarayanan, M. (2026) Nanocrystalline cookeite from lithium mineral deposits of Jammu, India: A multianalytical characterization. Earth Systems, Resources, and Sustainability, v.1(1), pp.97–109.

Sarma, D.S., McNaughton, N.J., Fletcher, I.R., Groves, D.I., Mohan, M.R. and Balaram, V. (2008) Timing of gold mineralization in the Hutti gold deposit, Dharwar craton, south India. Eco. Geol., v. 103, pp.1715–1727.

Satyanarayanan, M., Balaram, V., Sawant, S.S., Subramanyam, K.S.V., Krishna, G.V., Dasaram, B. and Manikyamba, C. (2018) Rapid determination of REEs, PGEs, and other trace elements in geological and environmental materials by high resolution inductively coupled plasma mass spectrometry. At. Spectrosc., v.39, pp.1–15.

Sawkar, R.H., Baldota, R., Suresh, S.R., Sastri, P.T., Kulgeri, A.S., Sarma, D.S., Subba Rao, D.V., Nirmalcharan, S. and Naqvi, S.M. (1999) Exploration, mine development and pilot plant operation at Gadag Gold Field, Karnataka, India. Journal of the Geological Society of India, v.54(3), pp.322–326.

Sindhuja, C.S., Satyanarayanan, M., Banerjee, S. and Chatterjee, S.

(2026) Geochemical and mineralogical constraints on lithium mineralization in rare-metal pegmatites of the Amareshwar region, Eastern Dharwar Craton, India. Geosystems and Geoenvironment, v.5, Article 100439.

Singh, T., Upadhyay, D. and Saha, R. (2026) Anatectic vs. granite-derived origin of pegmatites from the Bihar Mica Belt (eastern India): Insights from fluid inclusion and mineral chemistry, and Li-isotope composition of micas. Lithos, v.540–541, Article 108655.

Su, H., Wang, D., Wang, R., Yu, H., Zhang, W. and Guo, K. (2019) Global lithium resources and lithium-bearing pegmatites: A review. Acta Geologica Sinica (English Edition), v.93(Suppl. 1), pp.166–168.

Tenginkai, S.G. and Ugarkar, A.G. (1987) Gold-bearing rocks of Mangalur Greenstone Belt, Gulbarga District, Karnataka. Proceedings of the Indian Academy of Sciences (Earth and Planetary Sciences), v.96(2), pp.103–117.

Thillairaj, K. (2022) Detailed survey, geological mapping (1:2000) and bulk soil and rock sampling for assessing rare metal and rare earth potential of pegmatites and granitoids emplaced in Mangalur schist belt towards west of Mangalur and east of Kanahalli in Yadgir district, Karnataka. Unpublished Report, Atomic Minerals Directorate for Exploration and Research (AMD), Department of Atomic Energy, Hyderabad, 77p.

Thillairaj, K.K., Karmakar, P., Manthanwar, S.S.R., Gupta, P.P.K., Mundra, K.L. and Saravanan, B. (2024) A note on spodumene-bearing pegmatite of Chhotanagpur Granite Gneiss Complex, Garhtara–Dhangaon area, Korba district, Chhattisgarh. Current Science, v.127(2), pp.470–474.

Ugarkar, A.G. and Tenginkai, S.G. (1988) Gold–quartz–sulphide reefs of Mangalur, Gulbarga District, Karnataka. Current Science, v.57(3), pp.143–145.

Ugarkar, A.G. and Tenginkai, S.G. (1989) Mineragraphy of gold–quartz–sulphide reefs of the Mangalur Greenstone Belt, Karnataka. Journal of the Geological Society of India, v.33, pp.609–618.

Zozulya, D., Macdonald, R., Bagiński, B. and Jokubauskas, P. (2022). Nb/Ta, Zr/Hf and REE fractionation in exotic pegmatite from the Keivy province, NW Russia, with implications for rare-metal mineralization in alkali feldspar granite systems. Ore Geology Reviews. v.143, 104779. https://doi.org/10.1016/j.oregeorev.2022.104779